Relaxation of zonal flows in stellarators: influence of the magnetic configuration

E. Sánchez[1], P. Monreal[1], I. Calvo[1], R. Kleiber [2]

[1] *Laboratorio Nacional de Fusión, CIEMAT, 28040 Madrid, Spain*
[2] *Max Planck Institut für Plasmaphysik, D-17491, Greifswald, Germany*

The importance of zonal flows (ZFs) in the self regulation of turbulent transport is widely accepted nowadays. Although the ZF evolution is a nonlinear problem [1], involving the nonlinear drive and the collisional damping, studying its linear collisionless damping still provides valuable information [2]. In stellarators, in general, the linear collisionless relaxation of a zonal potential perturbation reaches a residual value after an oscillatory phase [3]. Two different characteristic oscillations, a geodesic acoustic mode (GAM) [4] and a low frequency oscillation (LFO), have been identified in stellarators depending on the magnetic configuration [5, 6]. There are indications that both, the ZF oscillations and the residual level, can affect plasma confinement [7, 8]. The residual ZF level as well as the oscillations depend on the radial scale of the perturbation and also on the magnetic configuration.

We take advantage of the flexibility of TJ-II [9] to scan different magnetic configurations and explore the influence of several configuration parameters (magnetic well, magnetic shear, magnetic field curvature and rotational transform) in the linear relaxation of ZFs. The magnetic shear is always very small in TJ-II, except in configurations with ohmic induced current. We have run linear gyrokinetic (GK) collisionless simulations of ZF relaxation with the code EUTERPE [10] for several radial wavelengths and several temperatures in a set of TJ-II configurations covering the ranges of variation in several parameters listed in the Table 1.

a	0.156 - 0.237 m
well	0.013 - 0.068
shear	0.008 - 0.118
ε_t	0.318 - 0.456
ι	1.178 - 2.231
$\langle\lvert\kappa_g\rvert\rangle$	0.589 - 0.734 m^{-1}
$\langle\lvert\kappa_n\rvert\rangle$	0.917 - 1.232 m^{-1}
$\langle\lvert\nabla s\rvert\rangle$	6.927 - 15.153 m^{-1}
k_Ψ	π - 6π
T	25 - 800 eV
$\langle k\rho\rangle$	0.035 - 0.152

Table 1: *Ranges of variation of several parameters in the TJ-II configurations studied.*

The simulations are done with adiabatic electrons and are initialized with a perturbation to the ion distribution function of the form $\delta f_i \propto \frac{\langle k_\perp^2 \rho_{ti}^2\rangle}{T}\sin(k_\psi s)F_M$ which produces a zonal potential perturbation, where F_M is a Maxwellian, ρ_{ti} is the thermal ion Larmor radius, T is the temperature, $k_\perp = k_\Psi|\nabla s|$ is the radial wavenumber of the perturbation and $\langle\rangle$ means flux surface average. The evolution of the radial electric field ($\phi'_{00}(t)$) is monitored at several radial positions, where ϕ_{00} is the $(0,0)$ Fourier component (in angle variables) of the potential and $'$ means derivative with respect to the radial

coordinate Ψ. In Fig. 1 a typical time evolution of the radial electric field (normalized to its initial value) is shown together with the Fourier spectrum of the time trace.

Two frequencies are clearly appreciated: a GAM oscillation that is damped very quickly and a LFO that lasts a longer time (see Fig. 1). From the Fourier spectrum the GAM amplitude and frequency is obtained. The LFO amplitude and frequency and the residual level can, in principle, be obtained from the spectrum, but the frequency resolution is poor compared to this frequency and a better result is obtained by fitting the time trace to a model $\frac{\phi'_{00}(t)}{\phi'_{00}(0)} = R + A_{LFO}\sin(\omega_{LFO}t)e^{\gamma t}$. The fit is also shown in Fig. 1. With this fit we obtain the residual ZF level, R, the ZF oscillation frequency, ω_{LFO}, and also an amplitude, A_{LFO}, and a damping rate, γ.

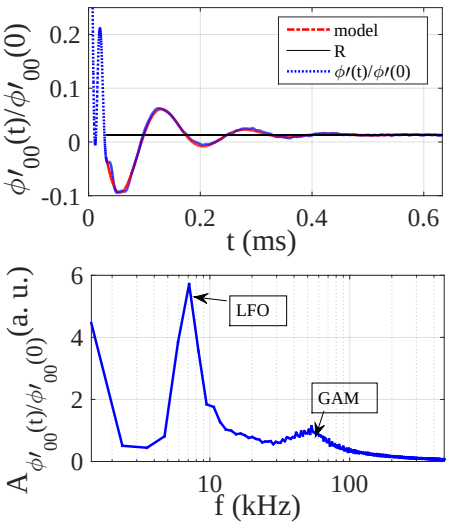

Figure 1: *Time trace (top) and spectra (bootom) of $\phi'_{00}(t)/\phi'_{00}(0)$ for a simulation in the TJ-II standard configuration with $k_\Psi = 3\pi$ and T=100 eV.*

We carried out a multivariate fit of A_{GAM}, ω_{GAM}, R, A_{LFO}, ω_{LFO} and γ with the magnetic configuration parameters. We complement the GK simulations with semi-analytical calculations of the residual ZF level with CAS3D-K [11, 3].

Residual level

In [3] the ZF residual level was studied for a wide range of radial wavelengths in the W7-X standard configuration by means of calculations with the code CAS3D-K and the results were compared to simulations with the GENE and EUTERPE GK codes. It was found that in the long-wavelength limit, and using the adiabatic electron approximation, $R = \frac{\phi'_{00}(\infty)}{\phi'_{00}(0)} \approx \frac{(1-\varepsilon_t)}{\langle k_\perp^2 \rho_{ti}\rangle^2 \varepsilon_t}$. That is, the residual level at a specific radial position depends only on three parameters: ε_t, the fraction of trapped particles at the flux surface, and $k_\perp$ and ρ_{ti}, defined previously.

It is expected that the details of the magnetic configuration affect the orbits of trapped particles and consequently the ZF residual. In particular, the geodesic curvature enters the radial magnetic drift and could affect it. We carried out a multivariate fit of the CAS3D-K calculations separately for the regions: $k_\perp\rho_{ti} < 0.2$, $0.2 < k_\perp\rho_{ti} < 1$ and $k_\perp\rho_{ti} > 1$. We found that the best fit of the residual in the long wavelength region ($k_\perp\rho_{ti} < 0.2$), including only $k_\perp\rho_{ti}$, ε_t, is $R \propto (k_\perp\rho_{ti})^{1.96\pm0.002}\varepsilon_t^{-1.46\pm0.01}$, close to $\langle k_\perp\rho_{ti}\rangle^2$. In the other regions the best fit is obtained including the averaged geodesic curvature $\kappa_G := \langle|\kappa_g|\rangle$ also. For $0.2 < k_\perp\rho_{ti} < 1$, the best fit is $R \propto (k_\perp\rho_{ti})^{0.88\pm0.01}\varepsilon_t^{-0.44\pm0.04}\kappa_G^{-1.80\pm0.15}$, and $R \propto (k_\perp\rho_{ti})^{-1.60\pm0.004}\varepsilon_t^{0.42\pm0.02}\kappa_G^{-2.45\pm0.07}$ for $k_\perp\rho_{ti} > 1$.

A multivariate fit of the results from GK simulations in the region with $k_\perp \rho_{ti} < 0.2$ gives as best fit $R \propto (k_\perp \rho_{ti})^{1.57\pm0.01} \varepsilon_t^{-1.69\pm0.04}$, with a slightly smaller dependency with $k_\perp \rho_{ti}$ as compared to the result obtained with CAS3D-K for the same scales. The long wavelength approximation used in EUTERPE for adiabatic electron simulations does not allow to study the region with $k_\perp \rho_{ti} > 0.5$ with this kind of simulations.

The influence of the trapped particles is much more important at large wavelengths, the corresponding exponent even changing sign for small wavelengths. A negative scaling of the residual with the geodesic curvature is obtained, the influence of κ_G on the residual being larger for small wavelengths. This result can be relevant if magnetic configuration optimization is pursued through reduction of the magnetic field curvature. The influence of curvature reduction on the residual level can be expected to be more important for small radial scales ZFs, produced by trapped electron mode turbulence, than for long wavelength ZFs from ion temperature gradient turbulence, typically in the range $k_\perp \rho_{ti} \sim 0.1$.

GAM oscillation

The GAM oscillation [4] is produced by the compression of the flux tubes at the high field side and expansion at the low field side. In a tokamak a clear dependency of the GAM frequency with q^{-1} is found. A dependency with $\sqrt{T_e + T_i}$ is also a characteristic of the GAM oscillation. In stellarators a similar dependency was found with T and q [5].

To study the scaling of GAM oscillation characteristics we analyze GK simulations for a set of magnetic configurations and carry out a multivariate fit of the GAM frequency and amplitude obtained from the Fourier spectrum. The best multivariate fit for the GAM frequency gives $\omega_{GAM} \propto T^{0.49\pm0.01} \iota^{0.45\pm0.04} \kappa_G^{0.85\pm0.13}$. Scalings of the frequency with T close to the typical with $\sqrt{T}$ and with q as $1/\sqrt{q}$ are found. An additional positive scaling with the geodesic curvature is found. This scaling is not surprising, as κ_G acts as the restoring force in the GAM. The scaling with κ_G is positive also in the amplitude.

For the oscillation amplitude the best fit gives $A_{GAM} \propto T^{-0.60\pm0.01} \iota^{0.030\pm0.06} \kappa_G^{0.46\pm0.17}$, with a scaling close to $1/\sqrt{T}$. The amplitude has low dependency with ι, in contrast to the result found for tokamaks and heliotrons, where the GAM damping rate scales with $1/q$.

Low frequency oscillation

The low frequency oscillation was studied in [6, 12] and was found to be related to the radial current produced by the radial drift of trapped particles.

From GK simulations in different TJ-II magnetic configurations we made a fit to the damped oscillation model obtaining the frequency, ω_{LFO}, the residual level, R, the amplitude, A_{LFO} and

the damping rate, γ, of the LFO. With these data we made a multivariate fit and got the scaling of these quantities with magnetic configuration parameters. It has to be taken into account that the model fitting is a subtle process and the fit is not always done properly so that some data have to be excluded from the analysis. The results of the multivariate fit are as follows:

For the LFO frequency we obtained $\omega_{LFO} \propto T^{0.50\pm0.02}\varepsilon_t^{0.57\pm0.09}\kappa_N^{1.26\pm0.12}\kappa_G^{-0.46\pm0.17}k_\perp^{0.15\pm0.02}$ as best fit. For the amplitude we get $A \propto T^{-0.52\pm0.03}\kappa_N^{1.57\pm0.20}\kappa_G^{-2.69\pm0.33}k_\perp^{-0.53\pm0.05}$ and for the damping rate $\gamma \propto T^{0.63\pm0.03}\varepsilon_t^{-0.33\pm0.13}\kappa_G^{3.11\pm0.34}k_\perp^{0.54\pm0.05}$.

A scaling close to $\sqrt{T}$ for the frequency and to $1/\sqrt{T}$ for the amplitude is found, as it was observed for the GAM oscillation. The damping increases with the temperature as in the case of the GAM oscillation. The frequency has a positive scaling with ε_t, as could be expected because the oscillation is produced by trapped particle's radial drift; consistently the damping rate has a negative scaling with ε_t. The frequency has almost no dependency with the radial scale of the perturbation ($k_\perp$) while it has a clear influence on the damping rate (positive exponent). The averaged normal curvature $\kappa_N := \langle|\kappa_n|\rangle$ has an effect opposite to that of κ_G on the oscillation frequency. Interestingly, the scaling of the frequency and amplitude with the geodesic curvature is opposite to that observed for the GAM oscillation and the damping rate is only affected by the geodesic curvature. The amplitude obtained in the fit is affected by the GAM oscillation.

Aknowledgement

This work has been partially funded by the Ministerio de Economía y Competitividad of Spain (project ENE2012-30832) and used resources from the Red Española de Supercomputación. We thank A. Könies for providing CAS3D-K. This work has been carried out within the framework of the EUROfusion Consortium and has received funding from the Euratom research and training programme 2014-2018 under grant agreement No 633053. The views and opinions expressed herein do not necessarily reflect those of the European Commission.

References

[1] P. H. Diamond, et. al., Plasma Phys. Control. Fusion **47**, R35-R161 (2005).
[2] M. N. Rosenbluth, and F. L. Hinton. Phys. Rev. Lett. **80** 724 (1998).
[3] P. Monreal, et al., submitted to PPCF (2015).
[4] N. Winsor, J. L. Johnson & J. M. Dawson. Phys. Fluids **11**, 11 (1968).
[5] H. Sugama, et al., Phys. Review Lett. **94** 115001 (2005).
[6] A. Mishchenko, et al., Phys. Plasmas **15**, 072309 (2008).
[7] M. Nunami, et al., Phys. Plasmas **20** 092307 (2013).
[8] P. Xanthopoulos, et al., Phys. Rev. Lett. **107** 245002 (2011).
[9] C. Alejaldre, et al., Plasma Phys. Control. Fusion, **41** A539-A548 (1999).
[10] G. Jost, et. al., Phys. Plasmas **7**, 1070664X (2001).
[11] A. Könies, et. al., Phys. Plasmas **7**, 1139 (2000).
[12] P. Helander, A. Mishchenko, R. Kleiber et al. Plasma Phys. Control. Fusion **53**, 5 (2011).